CrossMark

Head stabilization in a humanoid robot: models and implementations

Egidio Falotico[1] · Nino Cauli[1] · Przemyslaw Kryczka[2] · Kenji Hashimoto[3] ·
Alain Berthoz[5] · Atsuo Takanishi[4] · Paolo Dario[1] · Cecilia Laschi[1]

Abstract Neuroscientific studies show that humans tend to stabilize their head orientation, while accomplishing a locomotor task. This is beneficial to image stabilization and in general to keep a reference frame for the body. In robotics, too, head stabilization during robot walking provides advantages in robot vision and gaze-guided locomotion. In order to obtain the head movement behaviors found in human walk, it is necessary and sufficient to be able to control the orientation (roll, pitch and yaw) of the head in space. Based on these principles, three controllers have been designed. We developed two classic robotic controllers, an inverse kinematics based controller, an inverse kinematics differential controller and a bio-inspired adaptive controller based on feedback error learning. The controllers use the inertial feedback from a IMU sensor and control neck joints in order to align the head orientation with the global orientation reference. We present the results for the head stabilization controllers, on two sets of experiments, validating the robustness of the proposed control methods. In particular, we focus our analysis on the effectiveness of the bio-inspired adaptive controller against the classic robotic controllers. The first set of experiments, tested on a simulated robot, focused on the controllers response to a set of disturbance frequencies and a step function. The other set of experiments were carried out on the SABIAN robot, where these controllers were implemented in conjunction with a model of the vestibulo-ocular reflex (VOR) and opto-kinetic reflex (OKR). Such a setup permits to compare the performances of the considered head stabilization controllers in conditions which mimic the human stabilization mechanisms composed of the joint effect of VOR, OKR and stabilization of the head. The results show that the bio-inspired adaptive controller is more beneficial for the stabilization of the head in tasks involving a sinusoidal torso disturbance, and it shows comparable performances to the inverse kinematics controller in case of the step response and the locomotion experiments conducted on the real robot.

Keywords Humanoid robot · Head stabilization · Gaze stabilization · VOR · VCR

✉ Egidio Falotico
egidio.falotico@sssup.it

Nino Cauli
nino.cauli@sssup.it

Kenji Hashimoto
k-hashimoto@takanishi.mech.waseda.ac.jp

Alain Berthoz
alain.berthoz@college-de-france.fr

Atsuo Takanishi
takanisi@waseda.jp

Paolo Dario
paolo.dario@sssup.it

Cecilia Laschi
cecilia.laschi@sssup.it

[1] The BioRobotics Institute - Scuola Superiore Sant'Anna, Viale Rinaldo Piaggio, 34, 56025 Pontedera, PI, Italy

[2] Department of Advanced Robotics, Istituto Italiano di Tecnologia, via Morego 30, 16163 Genoa, Italy

[3] Faculty of Science and Engineering, Waseda University, 41-304, 17 Kikui-cho, Shinjuku-ku, Tokyo 162-0044, Japan

[4] Department of Modern Mechanical Engineering, Waseda University, 41-304, 17 Kikui-cho, Shinjuku-ku, Tokyo 162-0044, Japan

[5] LPPA/CNRS-Collège de France, 11 place Marcelin Berthelot, 75005 Paris, France

Springer

1 Introduction

1.1 Head stabilization in humans

In humans, the stabilization of the head in rotation creates a stable reference frame which may help the coordination of the body segments during locomotion (Pozzo et al. 1990, 1991). This unified inertial reference frame is centered on the head where a variety of sensory signals are integrated. Among them, the vestibular system located in the ear plays a major role in generating the sensory information necessary for the correct functioning of perception of the head movements and postures with respect to space and gravity. In this perspective, the head is an inertial guidance platform allowing human beings to acquire visual as well as vestibular information from a coherent and stable perception-based reference frame (Pozzo et al. 1990; Berthoz 2002). Pozzo et al. (1990) were the first ones to study the head behavior during locomotion. The main result of their experiments is that vertical translation of the head is partially stabilized during human walking. The head always rotates in the opposite direction from head translation along the vertical axis. This means that as the head translates up the head pitches down, and vice versa. Hirasaki et al. (1999) showed that the head oscillates up and down from about 4 cm during slow walking (0.8 m/s), to about 10 cm in fast walking (2 m/s), and about 5 cm from left to right in average in walking speeds between 1.4 and 1.8 m/s. A compensating contribution of the head yaw allows counteracting body (trunk) yaw to keep the orientation of the head stable. The same behavior has been observed for the roll and the pitch rotation of the head (Imai et al. 2001).

The head is not the only human segment to be stabilized. Indeed, the trunk segment is primarily responsible for regulating and attenuating gait-related oscillations between the lower trunk and head, with some additional assistance from the neck segment to stabilize the head at preferred and fast walking speeds (Kavanagh et al. 2006). Evidences from analysis of power spectral and amplitude characteristics of acceleration signals suggest that accelerations are also attenuated from the lower to upper trunk by the dynamics of the intervening trunk segment. They also suggest that the trunk segment plays an important role in modulating the structure of gait-related oscillations prior to reaching the head during gait. The variation of the head pitch angle is quite negligible with respect to other limbs orientation change. Therefore, as a first approximation Pozzo et al. concluded that in humans the orientation of the head is kept stable. Moreover, the head moves in translation in three directions. The reflex which uses vestibular information to stabilize head orientation in space is called angular vestibulo-collic reflex (aVCR) (Moore et al. 1999, 2001).

Keeping the head orientation fixed in space presents some advantages: the gaze is kept fixed on a distant target without intervention of eye muscles, and if the vestibular systems is kept aligned with the gravity vector the gravity-inertia ambiguity is reduced. In fact, looking more closely at the yaw and pitch rotation of the head, it can be seen that even if the magnitude of the head rotation with respect to the trunk is greatly reduced (Moore et al. 1999), they are not always stabilized accurately to a zero position: a correlation can be noticed between yaw and horizontal translation and in the same way between pitch and vertical translation. This kind of behavior can be explained if we suppose that the subject is looking at a fixed point located at some (small) distance ahead of his nose (Pozzo et al. 1990). When the head moves up in the vertical plane, pitch must compensate this movement by pointing down, and vice-versa. The same behavior must be followed also in the horizontal-yaw plane if we want to keep the gaze stable on a point ahead. This reflexive behavior which uses vestibular information to move the head to maintain the gaze on a point at a finite distance (and not parallel to itself as in aVCR) is called linear vestibulo-collic reflex (lVCR). Contributions from lVCR grow as speed increases. At speeds under 1.2 m/s the aVCR dominates, while at speeds above 1.2 m/s the lVCR is dominant (Hirasaki et al. 1999). Whether we want to stabilize the head in space or keep the head pointing at a fixed point, in both behaviors it appears clearly that the relevant degrees of freedom to be controlled are the angular ones. The behavior can then be implemented giving the suitable inputs to the controllers: zero in case of aVCR and some geometrically computable function of time for lVCR.

Walking with direction changes has been examined in Imai et al. (2001). Turning movements of both small radius (50 cm) and large radius (200 cm) have been captured at various speeds. One of the findings of this research is that large radius turns are in fact a combination of small radius turns and straight walking. So it is sufficient to analyze and replicate small-radius turning, in addition to straight walking treated previously. Considering small-radius turns, the main behaviors which are not present during straight walking are the yaw anticipation and roll anticipation. Analyzing the yaw data during turn, Imai et al. (2001) showed that head yaw is controlled (as it follows a smoother trajectory than body yaw) but it is not stabilized around trajectory yaw as we could expect. Head yaw anticipates heading and body yaw. In other words, subjects tend to turn their head towards the direction of the turn before the turn begins (Bernardin et al. 2012; Kadone et al. 2010). This kind of behavior is not generated by a feedback mechanism as it begins before the turn takes place. The roll is not stabilized to zero as it happens during straight walking. There is an anticipatory component of the roll in the direction of turning (i.e. the head tilts towards the inside of the turning trajectory). The magnitude of this

behavior, called roll anticipation, is not negligible: maximum roll is about 8 and there is a sustained roll component of approximately 5 during the main part of the turn (Imai et al. 2001). This behavior, moving the head towards the inside edge of the curve, creates a stabilizing moment with respect to the feet which helps to maintain balance during the turn (counteracting the outward weight shift caused by centrifugal forces).

Head stabilization and head anticipation of future events are two major requirements that need to coexist in the elaboration of the head motion command (Hicheur et al. 2005). This combination of stable and anticipatory head behavior is likely part of a gaze anchoring strategy combining both head and eye movements (Grasso et al. 1998). This is achieved in order to ensure a stable displacement of the whole body in the desired direction. It should be emphasized here that this anticipatory head behavior is still observed during blind-folded locomotion.

1.2 Head stabilization in robots

Despite the evidences for the importance of head stabilization in humans, robotics research do not address this issue widely. Farkhatdinov et al. (2011) were the first presenting the advantages of locating an IMU in the head of a humanoid robot. They assess that a stabilized robotic head would have the same benefits found in neuroscientific studies for the human beings, facilitating the estimation of the gravitational vertical. Based on the same neuroscientific principle of the head as an inertial guidance during locomotion, Sreenivasa et al. (2009) present successfull robot. The effect of head and trunk stabilization was also studied on passive walkers demostrating that the upper-body stabilization regulates naturally the walking limit cycle (Benallegue et al. 2013). In robotics literature, there are few implementations of head stabilization models (Yamada et al. 2007; Marcinkiewicz et al. 2009; Santos et al. 2009; Oliveira et al. 2011). Yamada et al. (2007) propose a method for the stabilization of the snake-like robot head based on the neck control. The aim of their controller is to reject the disturbance of the body on the head using a continuous model. Another work on the head stabilization implementation on a robotic platform is proposed in Santos et al. (2009) and Oliveira et al. (2011). This work focuses on a controller which minimizes the head motion induced by locomotion. In particular, the head movement is stabilized using a Central Pattern Generator and a genetic algorithm. The results on a Sony AIBO robotic platform show that the head movement is not totally eliminated during locomotion. Another controller (Marcinkiewicz et al. 2009) for the head stabilization has been implemented on the Sony AIBO robot. This controller is based on a machine learning algorithm able to learn the compensation for the head movements when no stabilization mechanism is present.

1.3 Rationale and objectives

In our research we focus on the development of a head stabilization algorithm for a humanoid robot. Considering the analysis of neuroscience findings in Sect. 1.1, we can conclude that in order to replicate head movement behaviors found in human walk it is necessary and sufficient to be able to control the orientation (roll, pitch and yaw) of the head in space. The described behaviors can be replicated by giving suitable references to the head orientation. Imposing an adequate reference for the head orientation can reproduce the anticipatory behavior described before for the curved path. A bio-inspired model (Falotico et al. 2011), based on these principles, has been proposed. It considers the trunk rotation as a disturbance and allows following an input reference head rotation, compensating the trunk rotation.

To realize the head orientation control, we developed two classic robotic controllers: an inverse kinematics based controller, an inverse kinematics differential controller (Kryczka et al. 2012a, b) and a bio-inspired controller based on feedback error learning (Falotico et al. 2012). In this paper we present a comparison of the results of the implementation of these algorithms on our humanoid platform SABIAN and on the simulator of the iCub robot. These algorithms use the feedback information from an Inertial Measurement Unit (IMU) to control the head orientation. Giving a suitable input to these controllers would allow to reproduce an anticipatory behavior in case of a curved trajectory [described in Hicheur et al. (2005) and Grasso et al. (1998)], but, in this work, we mainly focused on the stabilization capability. In fact we aim to assess the effectiveness of the controllers evaluating the capability of stabilizing the head in space (nullifying the rotation for roll pitch and yaw and compensating for the head translation imposing an appropriate reference for the head orientation).

In order to achieve this goal, we performed two sets of experiments. The first set of experiments, tested on a simulated robot, focused on the controllers response to a set of disturbance frequencies and a step function. The other set of experiments were carried out on the SABIAN robot, where these controllers were implemented in conjunction with a joint model of the vestibulo-ocular reflex (VOR) and opto-kinetic reflex (OKR) (Shibata and Schaal 2001; Franchi et al. 2010). Such a setup permits to compare the performances of the considered head stabilization controllers in conditions which mimic the human stabilization mechanisms composed of the joint effect of vestibulo-ocular reflex, opto-kinetic response and stabilization of the head. It is worth to notice that the main objective of this paper is not the evaluation of the VOR/OKR model performances, but instead the analysis of the performances of classic control methods (IJ and IK controllers) against

a bio-inspired adaptive controller (FEL controller) for the stabilization of the head. In particular we want to assess the effectiveness of the bio-inspired adaptive controller against the classic robotic controllers in order to define when this is more beneficial for the stabilization of the head.

The paper is organized as follows: in the next section we describe the controllers of head stabilization. The third section contains the description of the robotic platform. In the fourth section we describe the results of the experiments on the iCub Simulator and the SABIAN robotic platform and in last section we give a short summary and discussion of our results. In "Appendix 1" we describe the gaze stabilization model (including, OKR and VCR models) used to evaluate and to compare the head stabilization controllers on the SABIAN robot in terms of stabilization of the image.

2 Head stabilization controllers

We propose three different controllers. The first one is a differential kinematic controller (Kryczka et al. 2012a, b), the second one is an inverse kinematics controller and the last one is feedback error learning controller (Falotico et al. 2012).

We consider the first two controllers as classic robot controllers. The first one is a velocity-based approach with a feedback loop integrated in the operational space. This kind of controllers are more suitable for tasks where end-effector motion may be subject to online modifications in order to accommodate unexpected events or to respond to sensor inputs. The IK controller we designed, not being a velocity-based approach, should be less sensitive to noise. By integrating the feedback loop in the joint space, these controllers are able to follow the desired joint motion as closely as possible. The FEL model is a bio-inspired controller (Kawato 1990) which use an online learning network to learn the dynamics of the disturbance and a feedback loop implemented as a PD controller. As explained the control of the head rotation during walking appears essential in order to keep a stable head centered reference frame. In this perspective, a model in which the head is stabilized has been proposed by the authors (Falotico et al. 2011) which considers the trunk rotation as a disturbance and allows following an input reference head rotation, compensating the trunk rotation.

Three frames of reference are considered for this model: (1) the world reference frame $Oxyz$; (2) the head frame, fixed to the head, (3) and the trunk frame, fixed to the trunk. The head frame is composed by a rotation matrix $_H^W R$ which describes the orientation of the head with respect to the world frame as well as by a matrix $_H^T R$ which describes the orientation of the head with respect to the trunk. The trunk

frame orientation is composed by a rotation matrix $_T^W R$ which describes the orientation of the trunk with respect to the world frame. In this model, the matrix $_T^W R$ depends on the motion during walking and can be considered as an external disturbance which affects the $_H^W R$ matrix. The relation between these matrices is a composition of rotations:

$$_H^W R = {_T^W R} \, {_H^T R} \tag{1}$$

A controller was designed using as feedback the actual absolute roll, pitch and yaw (RPY) angles of the head (ν, ϕ, ψ), to track an arbitrary reference orientation in space (not relative to the trunk) using RPY angles. The controller is able to follow a reference orientation (ν^r, ϕ^r, ψ^r) spanning in the whole workspace of the head and reject the disturbance caused by trunk motion.

2.1 Inverse Jacobian (IJ) controller

For the implementation of this controller as a first solution we decided to use the spatial Jacobian. The spatial Jacobian of the head in an arbitrary configuration can be calculated using the rigid adjoint transformation of the direct kinematics. It can also be computed by direct inspection.

The Jacobian can be used to build a controller which has a proportional term k and a feed-forward term consisting of the derivative of the reference $(\dot{\nu}^r, \dot{\phi}^r, \dot{\psi}^r)$. We subtract a term consisting of the speed of trunk motion (disturbance) to compensate also for the trunk motion, because the composition of angular velocities is linear, unlike the composition of rotations. In order to obtain information about trunk motion, we can notice that, knowing the absolute orientation of the head $_H^W R$ and the orientation relative to the trunk $_H^T R$, we can estimate the rotation of the trunk,

$$_T^W R = {_H^W R} \left({_H^T R} \right)^{-1} \tag{2}$$

and then, by differentiation, we can obtain the time derivatives of the trunk RPY angles which can be used to compute the estimation of trunk orientation angles $\widehat{\nu}^t, \widehat{\phi}^t, \widehat{\psi}^t$ and their derivatives $\dot{\widehat{\nu}}^t, \dot{\widehat{\phi}}^t, \dot{\widehat{\psi}}^t$. The final control law becomes therefore:

$$\dot{\vartheta}_h^u(t) = J^{-1} \left(\begin{bmatrix} \dot{\nu}(t) \\ \dot{\phi}(t) \\ \dot{\psi}(t) \end{bmatrix} \right) \tag{3}$$

$$\dot{\nu}(t) = P_1(\nu^r(t) - \nu(t)) + \dot{\nu}^r(t) - \dot{\widehat{\nu}}^t(t)$$
$$\dot{\phi}(t) = P_2(\phi^r(t) - \phi(t)) + \dot{\phi}^r(t) - \dot{\widehat{\phi}}^t(t) \tag{4}$$
$$\dot{\psi}(t) = P_3(\psi^r(t) - \psi(t)) + \dot{\psi}^r(t) - \dot{\widehat{\psi}}^t(t)$$

where $J^{-1}()$ is the inverse Jacobian and P_1, P_2 and P_3 are proportional gains. Angular velocities of reference and trunk orientations are expressed in the inertial sensor reference frame.

The feedback controller is described in Fig. 1. The data available for the control are the current configuration of the joints and orientation of the head. The orientation is compared with the reference to compute the orientation error, while the joint configuration is used for forward kinematics calculation to obtain the trunk orientation. Based on the head orientation information it calculates the error between the head orientation reference and the current orientation. The error is further multiplied by the gain to obtain the velocity with which the head should be rotated to compensate for the error in a single control cycle. The head velocity information is further used in the inverse kinematics algorithm to calculate the neck joints velocity reference $\dot{\vartheta}_h^u$.

The system depicted in Fig. 1 denotes the robot with IMU mounted on the head. The information about the configuration is obtained from incremental encoders ϑ_h mounted on the motor shafts, while the head orientation in form of roll, pitch and yaw (ν, ϕ, ψ) is obtained from the IMU.

2.2 Inverse kinematics (IK) controller

Another way to build a controller is to use in some way the inverse kinematics relation. Given a reference absolute orientation matrix $_H^W R$ and an estimated torso orientation matrix we can compute the relative head rotation matrix which gives the desired orientation $_H^W R$ compensating exactly the torso motion. By solving the equation of the rotation composition obtaining the desired $_H^W R$

$$_H^T R = \left(_W^T R\right)^{-1} {}_H^W R \qquad (5)$$

with the computed $_H^T R$ we can find the joint angles which give that rotation matrix using the inverse kinematics formulae. The resulting control block is shown in Fig. 2.

As for the inverse Jacobian controller the orientation is compared with the reference to compute the orientation error, while the joint configuration is used for forward kinematics calculation to obtain the trunk orientation. The inverse kinematics module is used to compute the error in the joint space and this is sent to a PID controller replicated for the three
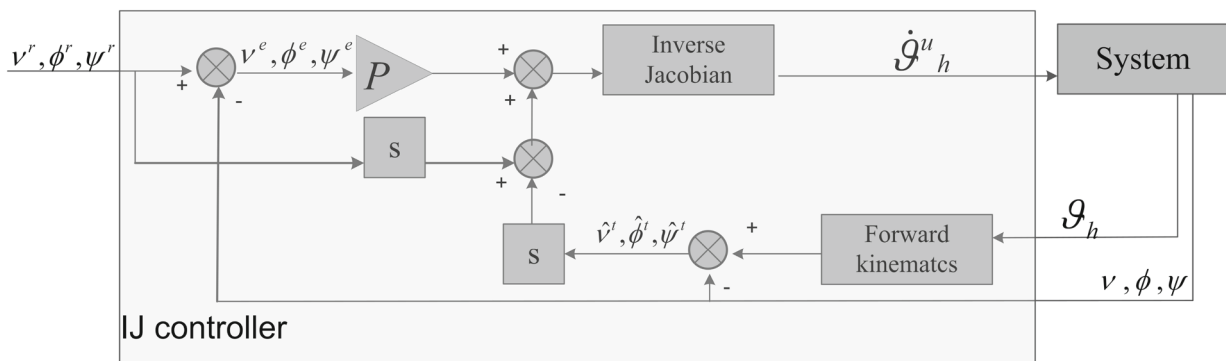

Fig. 1 A model of head stabilization based on the compensation of the trunk disturbance through an inverse Jacobian controller. This controller takes as input the head reference in the world coordinate space and yields the joint velocity of the robot neck. The feedback received from the system (the robot head) consists of the encoders values (ϑ_h) and the head orientation in form of roll, pitch and yaw (ν, ϕ, ψ) obtained from the IMU sensor
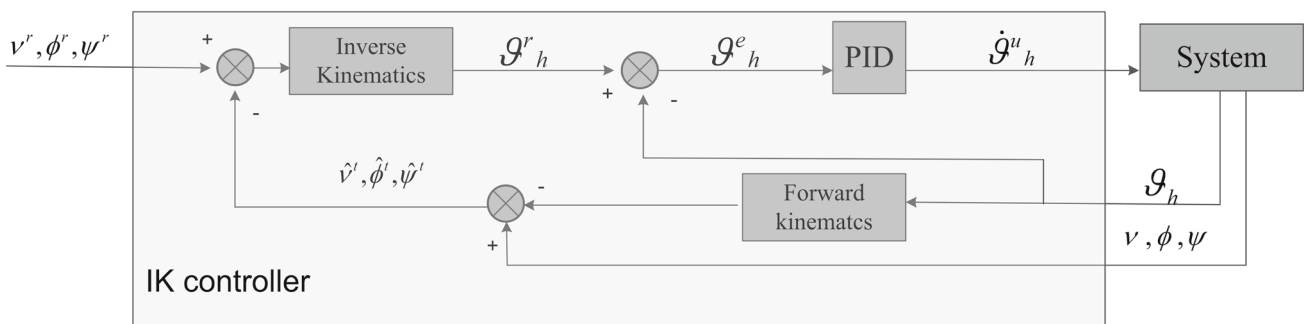

Fig. 2 A model of head stabilization based on an inverse kinematics controller. The model computes the error in the joint space and this is sent to a PID controller replicated for the three rotational axes which yields the joint velocities $(\dot{\vartheta}_h^u)$ for the robot neck
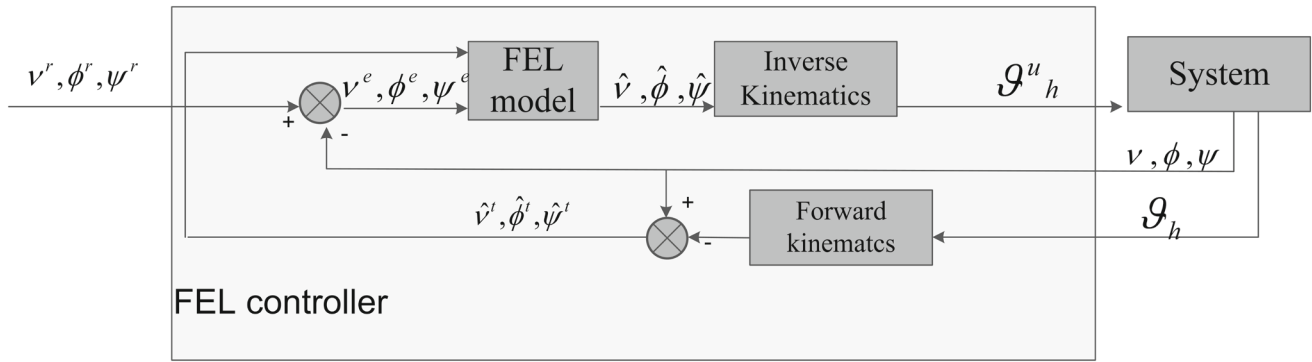
Fig. 3 A model of head stabilization based on a FEL controller. The model uses a learning controller in order to overcome the delays of the head motor system. The model yields the joint positions (ϑ_h^u) for the robot neck computing the error in the joint space which is the input of the FEL model (replicated for the three rotational axes)

rotational axes. This produces the joint velocity reference ($\dot{\vartheta}_h^u$). As for the previous controller the head configuration is obtained from the encoders ϑ_h, while the head orientation in form of roll, pitch and yaw (v, ϕ, ψ) is obtained from the IMU. In this case the control law equations are the following:

$$\dot{\vartheta}_h^u(t) = K_1(\vartheta_h^r(t) - \vartheta_h(t))$$
$$+ K_2 \int_0^t (\vartheta_h^r(\tau) - \vartheta_h(\tau))d\tau$$
$$+ K_3 \frac{d(\vartheta_h^r(t) - \vartheta_h(t))}{dt} \tag{6}$$

$$\vartheta_h^r(t) = k^{-1}\left(\begin{bmatrix} v^r(t) \\ \phi^r(t) \\ \psi^r(t) \end{bmatrix} - \left(\begin{bmatrix} v(t) \\ \phi(t) \\ \psi(t) \end{bmatrix} - k(\vartheta_h(t))\right)\right) \tag{7}$$

where $k()$ and $k^{-1}()$ are the forward and inverse kinematics functions and K_1, K_2 and K_3 are the PID gains.

2.3 Feedback error learning (FEL) Controller

The last controller we propose (see Fig. 3) is based on a feedback error learning model (FEL model) (Falotico et al. 2012). This model estimates the orientation of the head which allows following the reference orientation (v^r, ϕ^r, ψ^r). The output of this model is sent as input to an inverse kinematics module which computes the joint positions relative to the estimated orientation. The robot feedback is based on encoders and head rotations as for the other controllers. The learning controller takes as input the trunk orientation, its derivative and the orientation error. We replicate this model for each orientation (roll, pitch and yaw). In Fig. 4 we show the FEL model schema relative to the yaw. FEL employs an appropriate way of mapping sensory errors into motor errors (Kawato 1990; Falotico et al. 2012). The control law equations of the FEL controller are:
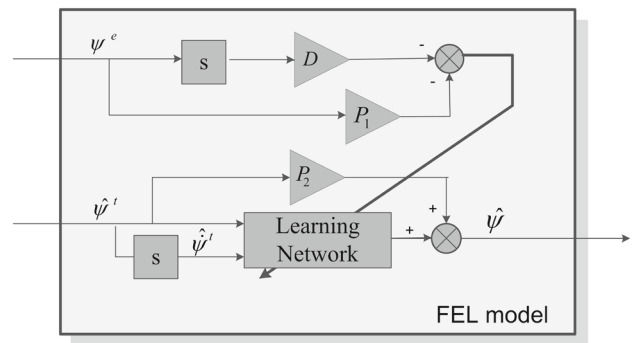

Fig. 4 The FEL controller implemented for the error learning of the yaw angular rotation

$$\vartheta_h^u(t) = k^{-1}\left(f_{FEL}\left(\begin{bmatrix} \widehat{v}^t(t) \\ \widehat{\phi}^t(t) \\ \widehat{\psi}^t(t) \end{bmatrix}, \begin{bmatrix} v^e(t) \\ \phi^e(t) \\ \psi^e(t) \end{bmatrix}\right)\right) \tag{8}$$

$$\begin{bmatrix} \widehat{v}^t(t) \\ \widehat{\phi}^t(t) \\ \widehat{\psi}^t(t) \end{bmatrix} = \begin{bmatrix} v(t) \\ \phi(t) \\ \psi(t) \end{bmatrix} - k(\vartheta_h(t)) \tag{9}$$

$$\begin{bmatrix} v^e(t) \\ \phi^e(t) \\ \psi^e(t) \end{bmatrix} = \begin{bmatrix} v^r(t) \\ \phi^r(t) \\ \psi^r(t) \end{bmatrix} - \begin{bmatrix} v(t) \\ \phi(t) \\ \psi(t) \end{bmatrix} \tag{10}$$

where $k()$ and $k^{-1}()$ are the forward and inverse kinematics functions and $f_{FEL}()$ is the FEL block function.

As a computationally learning mechanism, we use the recursive least squares (RLS) algorithm (Kawato 1990) for the learning network, introducing a small modification in the standard RLS algorithm. In the following, x is the state vector containing the angular position of the trunk (roll, pitch or yaw) and its derivative. To predict the angular position the model uses a second order linear system. The recursive least squares algorithm (RLS) is employed for learning, because it is robust and it guarantees fast convergence. The algorithm (for the yaw rotation) is as follows:

$$P(t) = \frac{1}{\lambda} \left[P(t-1) - \frac{P(t-1)x(t)x(t)^T P(t-1)}{\lambda + x(t)^T P(t-1)x(t)} \right]$$

$$\text{(11)}$$

$$\psi^e_{PD}(t) = -P_1\psi^e(t) - D\frac{d\psi^e(t)}{dt} \tag{12}$$

$$w(t) = w(t-1) + \frac{P(t)x(t)}{\lambda + x(t)^T P(t)x(t)}\psi^e_{PD}(t) \tag{13}$$

$$\widehat{\psi}(t) = w(t)^T x(t) + P_2\widehat{\psi}^t(t) \tag{14}$$

where P is the inverted covariance matrix of the input data, and λ is the forgetting factor which lies in the [0, 1] interval. For $\lambda = 1$, no forgetting takes place, while for smaller values, the oldest values in the matrix P are exponentially forgotten. The forgetting factor ensures that the prediction of RLS is only based on $1/(1-\lambda)$ data points.

3 Robotic platforms: iCub head and SABIAN biped humanoid

SABIAN (Sant'Anna BIped humANoid) is a biped humanoid robot developed by the Robot-An Laboratory, at Scuola Superiore Sant'Anna (see Fig. 5). It is a copy of WABIAN (WAseda BIped humANoid) (Ogura et al. 2006). The SABIAN robot (63.5 kg weight, 1.63 m height) has 7 DOF in each leg, 2 DOF in the waist, which help the robot perform stretched knee walking, 2 DOF in the trunk (for yaw and roll
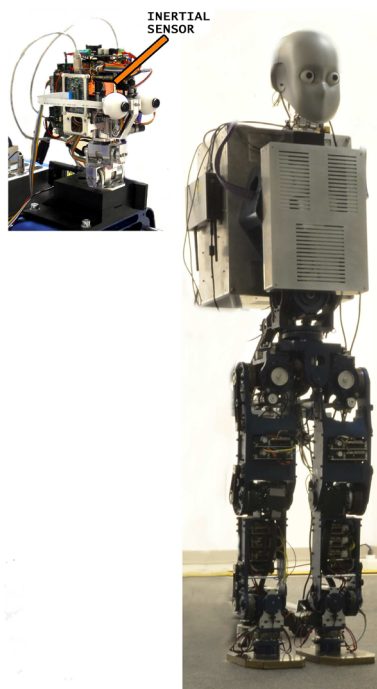

Fig. 5 The SABIAN humanoid robot (*right*) and the SABIAN head (*left*). The IMU sensor has been mounted in the center of the robot head

rotations). Every degree of freedom has a bio-inspired range of motion, defined in reference to human motion measurements. The computer mounted on the trunk controls the body motion. It consists of a PCI CPU board and PCI I/O boards. As the I/O boards, HRP interface boards (16ch D/As, 16ch counters, 16ch PIOs), and 6-axis force/torque sensor receiver board are mounted. The operating system is QNX Neutrino ver. 6.4. The drive system consists of a DC servo motor with an incremental encoder attached to the motor shaft, and a photo sensor to detect the basing angle. Each ankle has a 6-axis force/torque sensor, which is used for measuring Ground Reaction Force (GRF) and Zero Moment Point (ZMP). In order to reach the objectives of a gaze-guided locomotion, the iCub head (Beira et al. 2006) has been mounted on the SABIAN platform. The iCub head contains a total of 6 DOFs: 3 for the neck (pan, tilt and swing) and 3 for the eyes (an independent pan for each eye and a common tilt). The visual stereo system consists of 2 dragonfly2 cameras with a maximal resolution of 640X480 pixels. All the joints are actuated by DC servo motors with relative encoders. The processing unit consists of a PC104 with a Live Debian Distro running on it. An IMU is mounted on the iCub head, used as a source of the head absolute orientation information. The IMU sensor is an XSense MTx unit. It has an angular resolution of 0.05° with a repeatability of 0.2°. The roll and pitch static accuracy is 0.5° while the dynamic one is 2°. The IMU sensory data are sampled with a 100 Hz frequency. The sensor is mounted inside the SABIAN's head (see Fig. 5). The sensor yields absolute orientation information in terms of RPY angles. Since the head is equipped with big number of motors, which produce high electromagnetic field the readings of the IMU magnetic sensor are heavily affected. The magnetic sensor information is used inside the IMU algorithm to compensate for the drift of yaw angle. As a result of high unpredictable magnetic field, the yaw tends to drift. Since wrong yaw angle readings would affect the head stabilization control, we substitute the yaw feedback with head yaw angle calculated from forward kinematics. Since the angles mostly affected by the impacts are pitch and roll, this modification should not affect the main objective. Due to this limitation together with the lack of actuation in the trunk of the SABIAN robot, we performed a frequency test and a step response test on the iCub Simulator.

4 Experimental results

4.1 Tests of frequency response on the iCub Simulator

We implemented the three head stabilization controllers (IJ, IK and FEL) in the iCub Simulator to perform a controlled frequency test of the model in a platform having the same kinematics chain of the SABIAN's head. For these tests the

Table 1 Parameter values used for the implementation of the three controllers in the iCub Simulator and the SABIAN robot

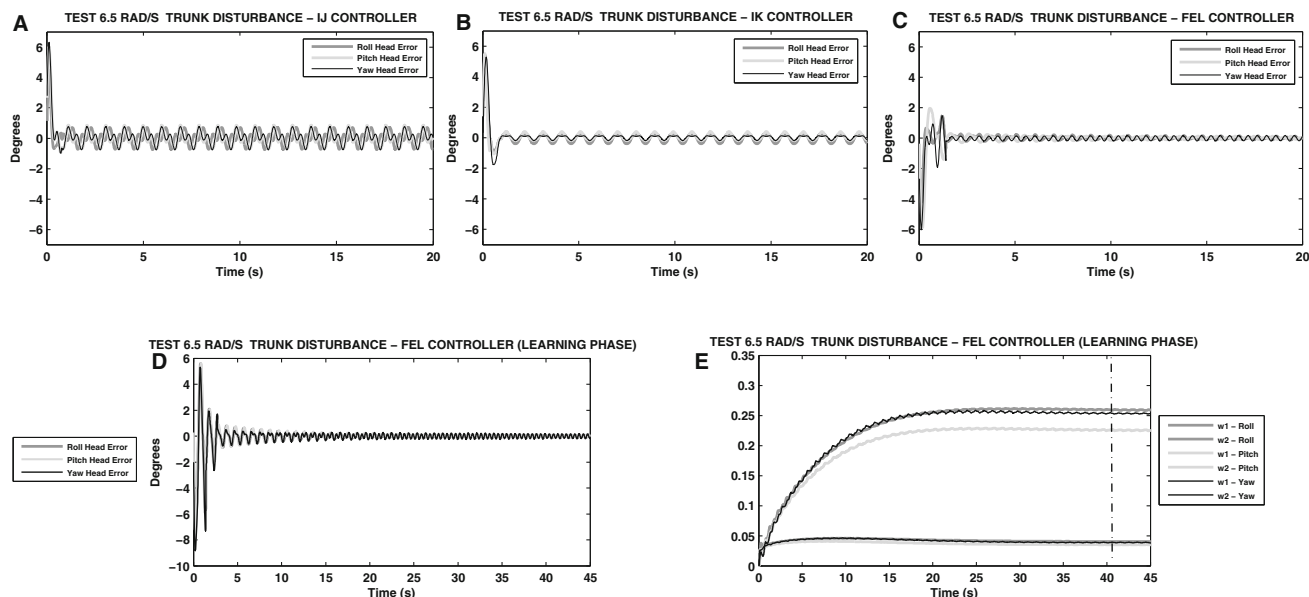| Parameter	iCub Simulator	SABIAN robot
P1, P2, P3 (IJ controller)	12, 12, 5	10, 10, 4
K1, K2, K3 (PID pitch IK controller)	30, 0.5, 0.1	20, 0.2, 0.1
K1, K2, K3 (PID roll IK controller)	30, 0.5, 0.1	20, 0.2, 0.1
K1, K2, K3 (PID yaw IK controller)	30, 0.5, 0.1	20, 0.2, 0.1
P1, P2, D, λ (pitch FEL controller)	0.1, 0.1, 0.01, 0.98	0.1, 0.1, 0.01, 0.995
P1, P2, D, λ (roll FEL controller)	0.1, 0.1, 0.01, 0.98	0.1, 0.1, 0.01, 0.995
P1, P2, D, λ (yaw FEL controller)	0.1, 0.1, 0.01, 0.98	0.1, 0.1, 0.01, 0.999

Fig. 6 Simulation results on the iCub Simulator in case of a sinusoidal trunk motion at 6.5 rad/s for the three proposed controllers (IJ, IK and FEL). **a** Head rotational error using the IJ controller. **b** Head rotational error using the IK controller. **c** Head rotational error using the FEL controller after the learning phase. **d** Time course for the learning phase of the FEL controller along the three rotational axes. **e** Regression parameter of the FEL controller during the learning phase. The *vertical dotted line* indicates the convergence time

same trunk perturbation has been applied to the three rotational axes:

$$x(t) = A * \sin(\omega * t) \tag{15}$$

where $x(t)$ is the trunk roll, pitch or yaw orientation (expressed in degrees) at the time t and A is the amplitude of the dynamics. The frequency (ω) has been tested between 0.5 and 12 rad/s (we increased the trunk frequency along the three rotational axes of 0.5 rad/s in each trial) with an amplitude of 20°. An inertial sensor is modelled in the iCub Simulator.

For this simulation we used the parameters listed in the Table 1, in the column named iCub Simulator, with the control loop running at 100 Hz. In order to determine the parameters listed in Table 1 we experimentally found the "best values" for such parameters at 4 sample disturbance frequencies (3, 6.5, 9.5, 12 rad/s) for the IK, the IJ and the

learning phase of the FEL controller. We then evaluate the controllers performances on all the considered disturbance frequencies (range 0.5–12 rad/s) using these 4 sets of "best values" in order to identify the best setup for each controller. We found that the best setup for the listed parameters is that one related to the 12 rad/s for the IK and the IJ controller and the 6.5 for the learning phase of the FEL controller. The reference value for roll, pitch and yaw rotation is constant and equal to 0. We executed 24 trials of 20 s (simulated time). We repeated this for the three controllers (IJ, IK and FEL). Figure 6 shows the error along the three rotational axes of a typical trial (trunk disturbance frequency 6.5 rad/s) for the three controllers (Fig. 6a–c). It should be noticed that, for the FEL model, the trials started with the regressor parameters of the FEL set to the values reached at the end of the training phases (Franchi et al. 2010). For the training phase we performed a task moving the trunk at a frequency of 6.5 rad/s
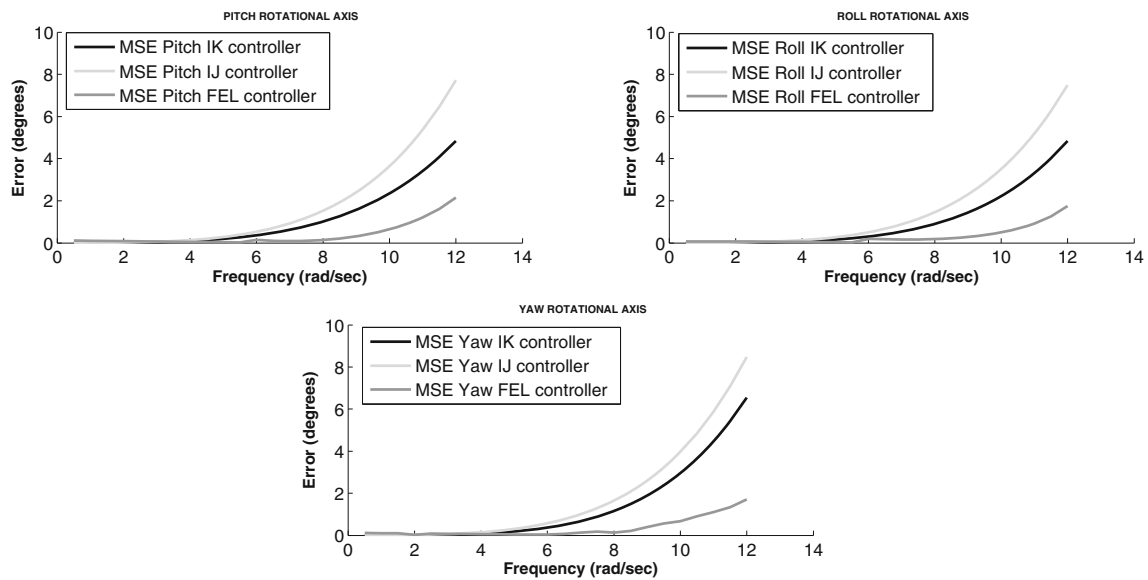
Fig. 7 Simulation results on the iCub Simulator in case of a sinusoidal trunk motion at several phases ranging from 0.5 to 12 rad/s for the three proposed controllers (IJ, IK and FEL). The FEL controller [with the regression parameters set to the value reached at the end of the training phase, as described in Franchi et al. (2010) and in the main text] seems to be phase invariant (for the considered phase range) unlike the IJ and the IK controller

(see Fig. 6d) until all the regressor parameters reached convergence (after 41 s of simulated time). We consider that the regression parameters stabilize when the peak-to-peak amplitude of the last 500 steps is less than 0.001 for both parameters of roll, pitch and yaw (see Fig. 6e). Figure 7 shows the mean square error (MSE) of the head rotation computed in each trial along the three rotational axes. The response of the IJ and the IK controller seems dependent on the increasing frequency. The IK controller has better performance compared to IJ along the three rotational axes. The FEL controller has better performance compared to the other controllers (the mean error never exceeds 2°), even if the error increases significantly as the disturbance frequency exceeds 8 rad/s.

4.2 Tests of step response on the iCub Simulator

For this simulation we used the parameters listed in the Table 1, in the column named iCub Simulator (as for the previous experiments). The trunk is placed at −10° along the three rotational axes before the beginning of the trial and the reference value for roll, pitch and yaw rotation is constant and equal to 0. Figure 8 shows the error along the three rotational axes for the three controllers responding to a step function. It should be noticed that, as for the previous set of experiments, for the FEL model, we show the results for the trial started with the regressor parameters set to the values reached at the end of the training phases (see Fig. 8c). The training phase is the same task executed with the regression parameters initial value set to 0 (see Fig. 8a). In order to eval-

uate the performances of the controllers we considered the following parameters: rise time, settling time, overshoot and peak time (Franklin et al. 2002). The rise time t_r is the time the system takes to reach the vicinity of the new reference point (in our case 10% of the step amplitude distance from the reference). The settling time t_s is the time the system takes to converge to a predefined interval around the new reference (in our case 1%). The overshoot M_p is the overshoot of the system compared to the new reference value (expressed as percentage). The peak time t_p is the time the system takes to reach the maximum overshoot point. The Table 2 shows the performance parameters value for the three controllers along the yaw rotational axis (we considered yaw being the axis along which the three controllers have worst performances). For the FEL model we present the results for the learning phase and after the learning. In terms of time (t_r, t_s and t_p) the FEL controller, in the trial after the learning phase, outperforms the other ones, even if the difference is restrained. In terms of overshoot, the IK controller has a better response to the step (2.88°) compared to IJ (4.12°) and FEL (4.22°).

4.3 Tests of the gaze stabilization model on the SABIAN robot

In this subsection we present the experiments performed on the SABIAN robotic platform. In order to run the IJ, IK and FEL controllers on the real robot we implemented a gaze stabilization model integrating VOR, OKR and the stabilization
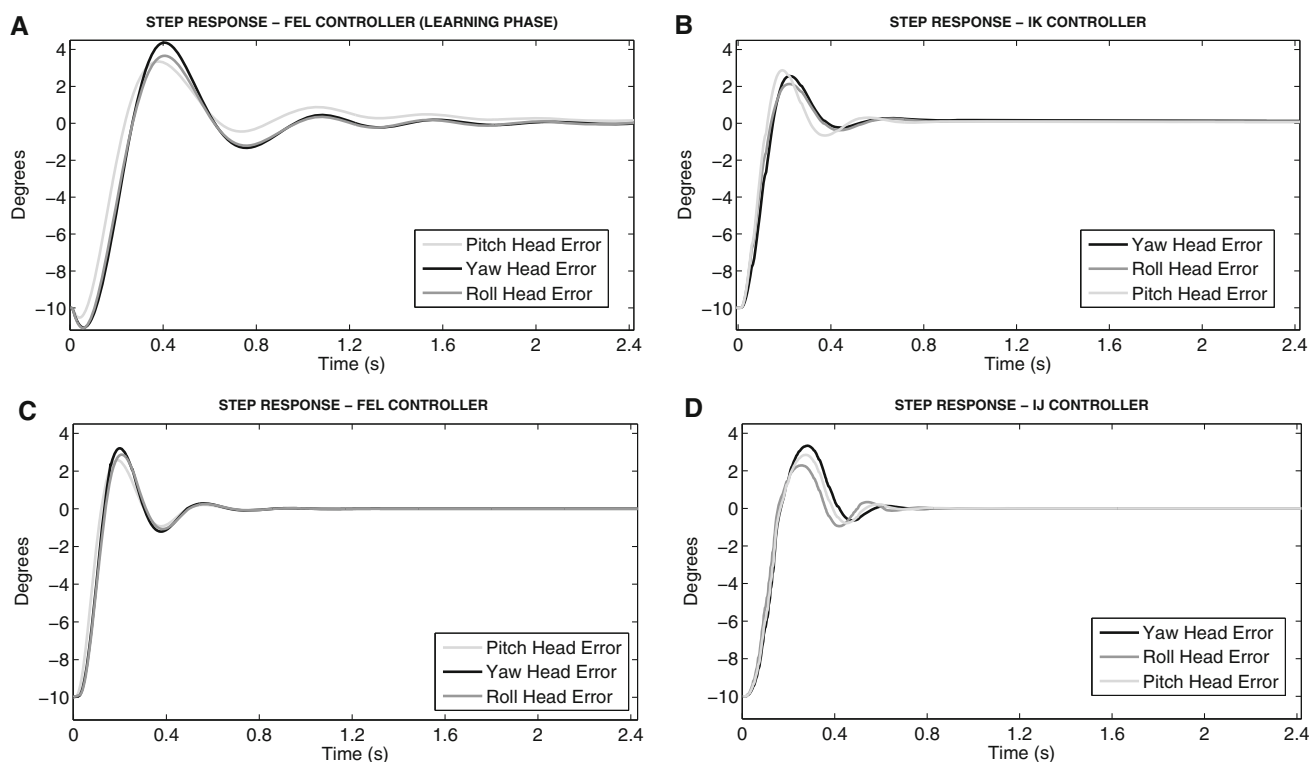
Fig. 8 Simulation results on the iCub Simulator in case of a step response for the implemented controllers. **a** Head rotational error using the FEL controller during the learning phase. **b** Head rotational error using the IK controller. **c** Head rotational error using the FEL controller after the learning phase. **d** Head rotational error using the IJ controller

Table 2 Parameters of the step response performance along the yaw axis for the considered controllers

Controller	t_r (s)	t_s (s)	M_p (%)	t_p (s)
FEL learning phase	0.35	0.55	56.1	2.22
IK	0.25	0.35	28.8	0.95
IJ	0.33	0.44	41.2	0.98
FEL after learning	0.23	0.32	42.2	0.88

controllers. This model has a twofold validation purpose for the proposed head stabilization controllers:

1. Show that the head stabilization controller gives a strong contribution in improving image stability during walking, allowing to increase the stabilization performance compared to the VOR/OKR system alone.
2. Allow to compare the performance of the considered head stabilization controllers in conditions which mimic the human stabilization mechanisms composed of the joint effect of VOR/OKR and stabilization of the head (VCR).

For the interested reader, we describe in details the model in "Appendix 1".

We performed a set of experiments verifying the algorithms effectiveness of decoupling an orientation movement of the head from rest of the body. For that purpose we considered an experimental scenario, the robot performed straight forward walk. The step length was 200mm, step width 180mm, step time 1s. In the single experiment the robot performed 10 steps. In all of the experiments robot was performing forward walk with stretched knee phase and flat foot initial contact. The vision system of the robotic head has two cameras with a resolution of 320x240 pixel and the frame rate of 60 fps. The OKR subsystem of the FEL and the Head Pointing module have an internal loop of 17 ms according to the camera frame rate, whilst the predictor and the VOR subsystem have a control loop of 10 ms as the head stabilization controllers (IJ, IK and FEL). We use a tracking algorithm based on particle filtering (Taiana et al. 2010) to evaluate the position error on the image and to computes the 3D position of the target. For these experiments we used the parameters listed in the Table 1, in the column named SABIAN robot. The listed parameters were chosen to optimize the performances of the controllers on a disturbance frequency of 6.28 rad/s, corresponding to the estimated trunk disturbance frequency during a walking task. The control system sends motor commands (joint position for
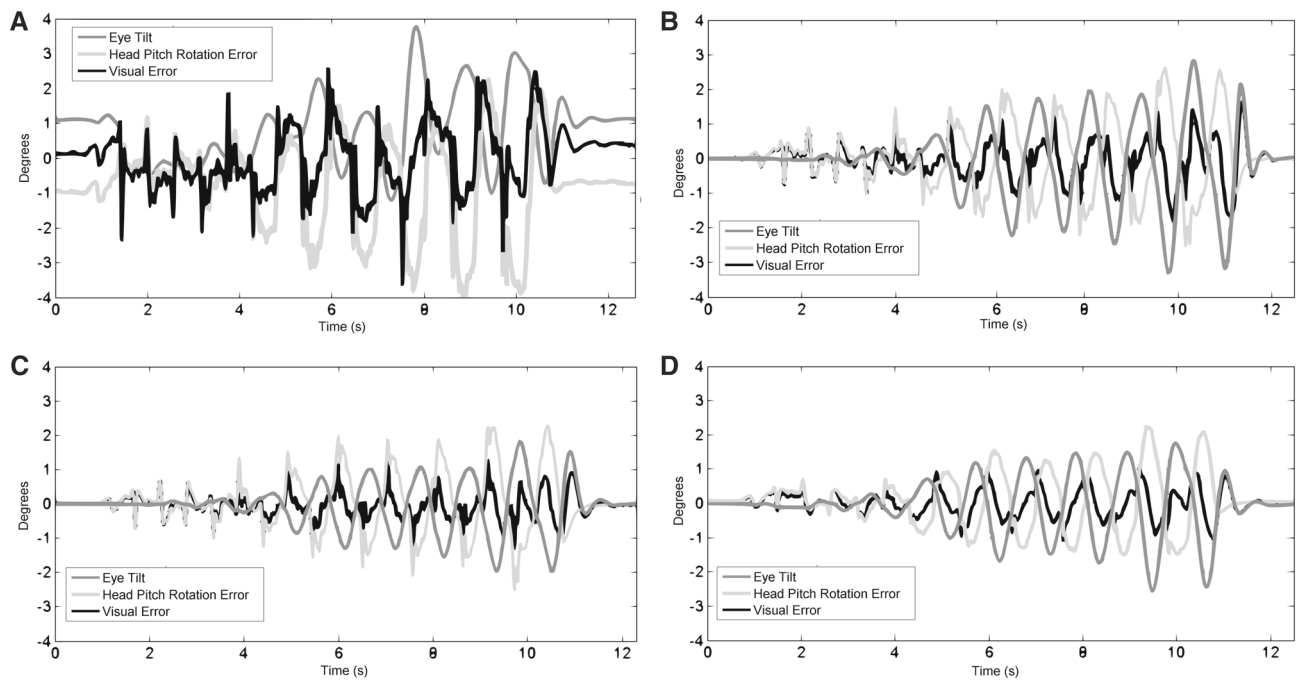
Fig. 9 Results on the SABIAN robot of the implementation of the proposed gaze stabilization model. The *graphs* show the results for the vertical plane considering the head pitch rotation error, the eye tilt rotation and the eye tilt rotation error (visual error). In order to assess the advantages of the implementation of the head stabilization model and to provide a comparison among the proposed controllers the robot performed the same walking trial in four different conditions: **a** no head stabilization controller active, **b** IJ controller active, **c** IK controller active and **d** FEL controller active

the FEL models of VOR/OKR and the FEL controller of the head and joint velocities for the IJ and the IK controller) by TCP/IP protocol using YARP ports, to the robot controller. Also for these experiments, for the FEL model of VCR and VOR/OKR, the trials started with the regressor parameters set to the values reached at the end of the training phase. For the training phase the robot performed thirty steps in a straight line (the step length was 100mm, step width 100mm, step time 1s). In order to assess the advantages of the implementation of the head stabilization model and the to provide a comparison among the proposed controllers the robot performed the same walking trial in four different conditions: (A) No head stabilization controller active, (B) IJ controller active, (C) IK controller active and (D) FEL controller active (see Fig. 9). Table 3 contains the results (MSE) for each trial (three for each condition) and their mean value for head pitch rotation error, head roll rotation error, visual error and retinal slip (derivative of the visual error).It should be noticed that there is a decrease of the visual error in case one of the three head stabilization controller is active. The FEL controller has better performance in head stabilization and visual error cancellation compared to the other controllers (the last row of the Table 3 shows the mean value across trials), even if the performance of the three controllers in this task are close to each other.

5 Conclusions

In this paper we presented the implementation of three controllers for head stabilization on a humanoid robot. We developed two classic robotic controllers (an inverse kinematics based controller and an inverse kinematics differential controller) and a bio-inspired adaptive controller based on feedback error learning.

These controllers are able to follow a reference orientation for the head rejecting the trunk disturbance, thus guaranteeing a stable orientation for the head during robot motion. We performed two sets of experiments validating the effectiveness of the proposed control methods. The first set was conducted on the simulator of the iCub robot to test the controllers response to a set of disturbance frequencies and a step function.

The other set of experiments were carried out on the SABIAN robot to show the improvements in the head stabilization (for pitch and roll rotation) during locomotion. The results show that while walking the robot head, for the roll and the pitch rotation in the global reference frame, appears stable, differently from the case of working without our control systems. The above results proved that the proposed controllers can be used to stabilize the head of the humanoid robot during locomotion. This is very helpful in gaze-guided

Table 3 Results on the SABIAN robot of the implementation of the proposed gaze stabilization model

	OKR+VOR				OKR+VOR+VCR (IJ)				OKR+VOR+VCR (IK)				OKR+VOR+VCR (FEL)			
	HPE (°)	HRE (°)	VE (°)	RS (°/s)	HPE (°)	HRE (°)	VE (°)	RS (°/s)	HPE (°)	HRE (°)	VE (°)	RS (°/s)	HPE (°)	HRE (°)	VEdeg	RS (°/s)
TR.1	0.94	0.9	0.35	0.62	0.43	0.29	0.15	0.49	0.38	0.27	0.12	0.48	0.36	0.27	0.11	0.44
TR.2	1.04	0.94	0.38	0.69	0.38	0.28	0.14	0.50	0.37	0.25	0.12	0.45	0.34	0.25	0.11	0.47
TR.3	0.98	0.93	0.37	0.68	0.41	0.29	0.18	0.52	0.38	0.28	0.14	0.49	0.38	0.28	0.12	0.44
Mean	0.99	0.92	0.37	0.66	0.41	0.29	0.16	0.50	0.38	0.27	0.13	0.47	0.36	0.27	0.12	0.45

The four columns provide a comparison for the results in the four considered conditions: No head stabilization controller active, IJ controller active, IK controller active and FEL controller active. The table contains the results (MSE) for each trial (three for each condition) for head pitch rotation error (HPE), head roll rotation error (HRE), visual error (VE), retinal slip (RS) which is the derivative of the visual error

locomotion tasks because it helps the gaze stabilization facilitating the VOR, as confirmed by our walking experiment.

In this paper we wanted also to evaluate the effectiveness of the bio-inspired FEL controller against the two classic robotic controllers. The FEL controller has better performances in the iCub Simulator tests on sinusoidal disturbances compared to the other controllers and slightly better performances in terms of settling time, rise time and peak time in the step response task. Considering the tests on the SABIAN robot, the results of the FEL controller are close to those produced by the IK controller. This is probably due to the impulsive acceleration the robot head, while walking, is subjected to. The impact due to the foot initial contact with the ground is strong enough to disturb the controller and cause the head orientation to deviate from the reference. A possible improvement could concern the replacement of the learning network in the FEL model in order to compensate for these impulsive accelerations. The results obtained in head stabilization lead to another important study, concerning walking on soft ground. Walking on soft ground has different effects as shown by MacLellan and Patla (2006a), MacLellan and Patla (2006b), Kang et al. (2012) and Hashimoto et al. (2012).

The trunk perturbation as well as the head translation (mostly in the vertical plane) change in frequency and amplitude to support step adaptation and stable posture during locomotion. The head stabilization controllers presented here can compensate for such changes and ensures a stable head orientation on soft ground, too.

Appendix 1: A model of gaze stabilization

In this appendix we present a complete gaze stabilization model that we used to run the IJ, IK and FEL controllers on the real robot. In humans one of the objectives of the head stabilization mechanism is to keep the image stable on the retina. Vision is degraded if an image slips on the retina, so stabilizing images is an essential task during everyday activities. Among the different mechanisms used to stabilize vision, the vestibulo-ocular reflex (VOR) is certainly the most important. The VOR compensates for head movements that would perturb vision by turning the eye in the orbit in the opposite direction of the head movements (Barnes 1993). VOR works in conjunction with the opto-kinetic response, which is a feedback mechanism that ensures that the eye moves in the same direction and at almost the same speed as
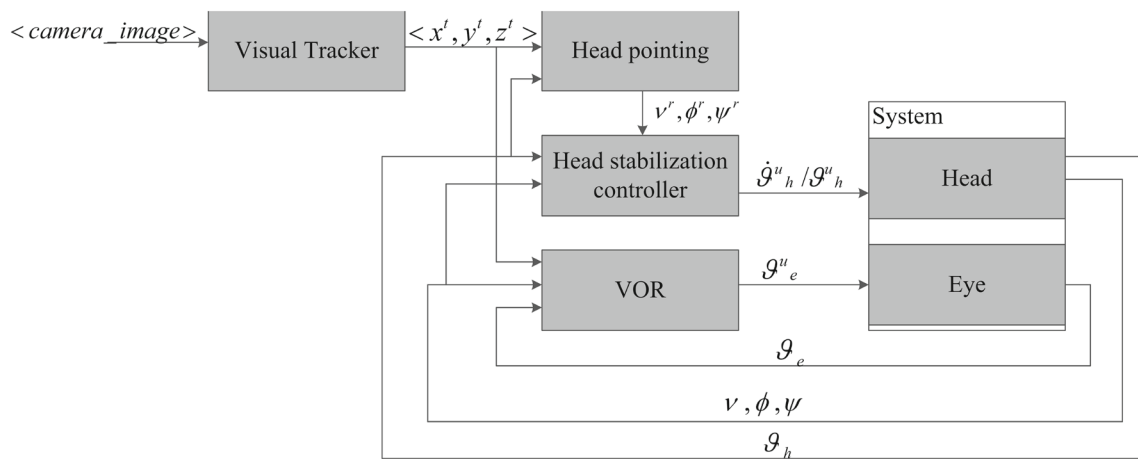
Fig. 10 A model of gaze stabilization. This model aims to reproduce the joint effect of VCR for the head stabilization and the VOR and OKR for the image stabilization (Shibata and Schaal 2001; Shibata et al. 2001). We added a module named Head Pointing in order to guarantee the head contributes to center the target compensating during locomotion for the head translations. The model takes as input the target position in the camera image and computes the neck and eye joints position (or velocity)

an image. Together, VOR and OKR keep the image stationary on the retina, with VOR compensating for fast movements and OKR for slower ones (Schweigart et al. 1997).

Several approaches have been used to model the VOR depending on the goal of the study. For our purpose we need a bio-inspired model of image stabilization through eye movements suitable for a robotic implementation. In the robotic literature we found some controllers inspired by the VOR implemented on a humanoid platform (Viollet and Franceschini 2005; Porrill et al. 2004; Shibata and Schaal 2001), but only the Schall's model replicates also the OKR mechanism. In particular it investigates the cooperation between these two ocular movements. OKR receives a sensory input (the retinal slip), which can be used as a positional error signal, and its goal is to keep the image still on the retina. VOR uses instead, as sensory input, the head velocity signal (acquired by the vestibular organs in the semicircular canals), inverts the sign of the measured head velocity and, with the help of a well-tuned feedforward controller, rapidly generates the appropriate motor commands for the eyes. In our implementation we use as input for the model the head rotation and the visual error on the camera image. To achieve appropriate VOR–OKR performance, the authors of the model synthesize the VOR system as a feedforward open-loop controller using an inverse control model. The OKR is defined instead as a compensatory negative feedback controller for the VOR, involving the PD controller based on retinal slip. These two systems form what is called the direct pathway of oculomotor control in biology. According to Shibata and Schaal (2001) and Shibata et al. (2001), to accomplish excellent VOR and OKR performance, it is necessary to introduce an indirect pathway. It corresponds to a learning network located in the primate cerebellum. It acquires during the course of learning an inverse dynamic model of the oculomotor plant. The learning controller takes as input the head velocity and the estimated position of the oculomotor plant and outputs necessary torque. It is trained with the FEL (feedback-error-learning) strategy. For successful FEL, the time alignment between input signals and feedback-error signal is theoretically crucial. To solve this problem the authors suggest the concept of eligibility traces, and model them as a second order linear filter of the input signals to the learning system.

The model of gaze stabilization we propose (see Fig. 10) takes the input from the camera image, computes the visual error (i.e. the distance from the center of the image) and the 3D position of the target and sends these values to a module of head pointing and to the VOR/OKR controller. The objective of the Head Pointing module is to center the target in the camera image controlling the neck joints. This allows also to compensate for the translations of the head in locomotion tasks. The output of this module is the reference of the head stabilization controller. The Head Pointing module computes the joints angles to point the target and convert them in an angular rotation of the head. In order to calculate the head inverse kinematics to point a tracked object, a Feedforward Multilayer Perceptron network has been implemented. The network has one hidden layer of 20 units. It takes as input the object 3D positions in the left eye reference frame (x^t, y^t, z^t) and as output the neck pitch and yaw joints angles. The network was trained offline in a simulated environment (Matlab SIMULINK). A 18,000 element random dataset, obtained using the direct kinematics, was used to train the network. The dataset outputs were created choosing 18,000 random values (from $-\pi/4$ to $\pi/4$) for the neck joints. From these values we computed the head rotation through the direct kinematics function to generate the angular rotation of the head

which is the output of the Head Pointing module. The dataset inputs were the 3D position of the object obtained using the following two steps:

– for each output head rotation, the roto-traslation matrix was calculated from the eye to the neck reference frame using Denavit–Hartenberg method
– the forward kinematics matrix was multiplied by the vector $E(0, 0, z)$, where the z was a random value between 100 and 5000 mm

The dataset was divided in training (70 %), validation (15 %) and test set (15 %). After 634 epochs, the test MSE error was around 0.0003 rad. For the robot experiments a trained network has been implemented in C++. The Head stabilization taking as input the reference (ν^r, ϕ^r, ψ^r) from the Head Pointing yields joint velocities or positions (depending on the controller). The VOR module takes as input the encoder value of the eye joints (ϑ_e) and the head rotation for the pitch or the yaw and produces the corresponding compensatory position movement of the eye joints (ϑ_e^u) along the same axis (eye vergence for the horizontal plane and eye tilt for the vertical plane).

References

Barnes, G. (1993). Visual–vestibular interaction in the control of head and eye movement: The role of visual feedback and predictive mechanisms. *Progress in Neurobiology*, *41*(4), 435–472.

Beira, R., Lopes, M., Praga, M., Santos-Victor, J., Bernardino, A., Metta, G., et al. (2006). Design of the robot-cub (icub) head. In *2006 IEEE international conference on robotics and automation (ICRA)* (pp. 94–100).

Benallegue, M., Laumond, J. P., & Berthoz, A. (2013). Contribution of actuated head and trunk to passive walkers stabilization. In *2013 IEEE international conference on robotics and automation (ICRA)* (pp. 5638–5643).

Bernardin, D., Kadone, H., Bennequin, D., Sugar, T., Zaoui, M., & Berthoz, A. (2012). Gaze anticipation during human locomotion. *Experimental Brain Research*, *223*(1), 65–78.

Berthoz, A. (2002). *The brain's sense of movement*. Cambridge: Harvard University Press.

Falotico, E., Laschi, C., Dario, P., Bernardin, D., & Berthoz, A. (2011). Using trunk compensation to model head stabilization during locomotion. In *2011 11th IEEE-RAS international conference on humanoid robots (Humanoids)* (pp. 440–445).

Falotico, E., Cauli, N., Hashimoto, K., Kryczka, P., Takanishi, A., Dario, P., et al. (2012). Head stabilization based on a feedback error learning in a humanoid robot. In *2012 IEEE International conference on proceedings—IEEE international workshop on robot and human interactive communication* (pp. 449–454).

Farkhatdinov, I., Hayward, V., Berthoz, & A. (2011). On the benefits of head stabilization with a view to control balance and locomotion in humanoids. In *2011 IEEE-RAS international conference on humanoid robots (Humanoids)* (pp. 147–152).

Franchi, E., Falotico, E., Zambrano, D., Muscolo, G. G., Marazzato, L., Dario, P., et al. (2010). A comparison between two bio-inspired adaptive models of vestibulo-ocular reflex (VOR) implemented on the iCub robot. In *2010 10th IEEE-RAS international conference on humanoid robots (Humanoids)* (pp. 251–256).

Franklin, G. F., Powell, J. D., & Emami-Naeini, A. (2002). *Feedback control of dynamic systems*. Upper Saddle River: Prentice Hall.

Grasso, R., Prévost, P., Ivanenko, Y. P., & Berthoz, A. (1998). Eye–head coordination for the steering of locomotion in humans: An anticipatory synergy. *Neuroscience Letters*, *253*(2), 115–118.

Hashimoto. K., Kang, H. J., Nakamura, M., Falotico, E., Lim, H. O., Takanishi, A., et al. (2012). Realization of biped walking on soft ground with stabilization control based on gait analysis. In *2012 IEEE/RSJ international conference on intelligent robots and systems (IROS)* (pp. 2064–2069).

Hicheur, H., Vieilledent, S., & Berthoz, A. (2005). Head motion in humans alternating between straight and curved walking path: Combination of stabilizing and anticipatory orienting mechanisms. *Neuroscience Letters*, *383*(1), 87–92.

Hirasaki, E., Moore, S. T., Raphan, T., & Cohen, B. (1999). Effects of walking velocity on vertical head and body movements during locomotion. *Experimental Brain Besearch*, *127*(2), 117–130.

Imai, T., Moore, S. T., Raphan, T., & Cohen, B. (2001). Interaction of the body, head, and eyes during walking and turning. *Experimental Brain Research*, *136*(1), 1–18.

Kadone, H., Bernardin, D., Bennequin, D., & Berthoz, A. (2010). Gaze anticipation during human locomotion—Top–down organization that may invert the concept of locomotion in humanoid robots. In *2010 IEEE international conference on international symposium in robot and human interactive communication* (pp. 552–557).

Kang, H. J., Hashimoto, K., Nishikawa, K., Falotico, E., Lim, H. O., Takanishi, A., et al. (2012). Biped walking stabilization on soft ground based on gait analysis. In: *2012 4th IEEE RAS EMBS international conference on biomedical robotics and biomechatronics (BioRob)* (pp. 669–674).

Kavanagh, J., Barrett, R., & Morrison, S. (2006). The role of the neck and trunk in facilitating head stability during walking. *Experimental Brain Research*, *172*(4), 454–463.

Kawato, M. (1990). Feedback-error-learning neural network for supervised motor learning. *Advanced Neural Computers*, *6*(3), 365–372.

Kryczka, P., Falotico, E., Hashimoto, K., Lim, H., Takanishi, A., Laschi, C., et al. (2012a). Implementation of a human model for head stabilization on a humanoid platform. In *2012 4th IEEE RAS EMBS international conference on biomedical robotics and biomechatronics (BioRob)* (pp. 675–680).

Kryczka, P., Falotico, E., Hashimoto, K., Lim, H. O., Takanishi, A., Laschi, C., et al. (2012b). A robotic implementation of a bio-inspired head motion stabilization model on a humanoid platform. In *2012 IEEE/RSJ international conference on intelligent robots and systems (IROS)* (pp. 2076–2081).

MacLellan, M. J., & Patla, A. E. (2006a). Adaptations of walking pattern on a compliant surface to regulate dynamic stability. *Experimental Brain Research*, *173*(3), 521–530.

MacLellan, M. J., & Patla, A. E. (2006b). Stepping over an obstacle on a compliant travel surface reveals adaptive and maladaptive changes in locomotion patterns. *Experimental Brain Research*, *173*(3), 531–538.

Marcinkiewicz, M., Kaushik, R., Labutov, I., Parsons, S., & Raphan, T. (2009). Learning to stabilize the head of a quadrupedal robot with an artificial vestibular system. In *2009 IEEE international conference on robotics and automation (ICRA)* (pp. 2512–2517).

Moore, S. T., Hirasaki, E., Cohen, B., & Raphan, T. (1999). Effect of viewing distance on the generation of vertical eye movements during locomotion. *Experimental Brain Research*, *129*(3), 347–361.

Moore, S. T., Hirasaki, E., Raphan, T., & Cohen, B. (2001). The human vestibulo-ocular reflex during linear locomotion. *Annals of the New York Academy of Sciences*, *942*(1), 139–147.

Ogura, Y., Aikawa, H., Shimomura, K., Morishima, A., Lim, H. O., & Takanishi, A. (2006). Development of a new humanoid robot

wabian-2. In *2006 IEEE international conference on robotics and automation (ICRA)* (pp. 76–81).

Oliveira, M., Santos, C. P., Costa, L., Rocha, A., & Ferreira, M. (2011). Head motion stabilization during quadruped robot locomotion: Combining CPGs and stochastic optimization methods. *International Journal of Natural Computing Research (IJNCR)*, *2*(1), 39–62.

Porrill, J., Dean, P., & Stone, J. V. (2004). Recurrent cerebellar architecture solves the motor-error problem. *Proceedings of the Royal Society of London-B*, *271*(1541), 789–796.

Pozzo, T., Berthoz, A., & Lefort, L. (1990). Head stabilization during various locomotor tasks in humans. *Experimental Brain Research*, *82*(1), 97–106.

Pozzo, T., Berthoz, A., Lefort, L., & Vitte, E. (1991). Head stabilization during various locomotor tasks in humans. *Experimental Brain Research*, *85*(1), 208–217.

Santos, C., Oliveira, M., Rocha, A. M. A., & Costa, L. (2009). Head motion stabilization during quadruped robot locomotion: Combining dynamical systems and a genetic algorithm. In *2009 IEEE international conference on robotics and automation (ICRA)* (pp. 2294–2299).

Schweigart, G., Mergner, T., Evdokimidis, I., Morand, S., & Becker, W. (1997). Gaze stabilization by optokinetic reflex (OKR) and vestibulo-ocular reflex (VOR) during active head rotation in man. *Vision Research*, *37*(12), 1643–1652.

Shibata, T., & Schaal, S. (2001). Biomimetic gaze stabilization based on feedback-error-learning with nonparametric regression networks. *Neural Networks*, *14*(2), 201–216.

Shibata, T., Vijayakumar, S., Conradt, J., & Schaal, S. (2001). Biomimetic oculomotor control. *Adaptive Behavior*, *9*(3–4), 189–207.

Sreenivasa, M. N., Souères, P., Laumond, J. P., & Berthoz, A. (2009). Steering a humanoid robot by its head. In *2009 IEEE/RSJ international conference on intelligent robots and systems (IROS), IEEE* (pp. 4451–4456).

Taiana, M., Santos, J., Gaspar, J., Nascimento, J., Bernardino, A., & Lima, P. (2010). Tracking objects with generic calibrated sensors: An algorithm based on color and 3d shape features. *Robotics and Autonomous Systems*, *58*(6), 784–795.

Viollet, S., & Franceschini, N. (2005). A high speed gaze control system based on the vestibulo-ocular reflex. *Robotics and Autonomous Systems*, *50*(4), 147–161.

Yamada, H., Mori, M., & Hirose, S. (2007). Stabilization of the head of an undulating snake-like robot. In *2007 IEEE/RSJ international conference on intelligent robots and systems (IROS)* (pp. 3566–3571).

Egidio Falotico is a Postdoctoral Researcher at The BioRobotics Institute, Scuola Superiore Sant'Anna (SSSA) in Pondedera. He received B.S. and M.S. degrees in Computer Science at the University of Pisa, Italy, in 2005 and 2008, respectively. He received the Ph.D. degree in Biorobotics and the Ph.D. degree in Cognitive Science (March 2013). His Ph.D. thesis was in co-tutoring between Scuola Superiore Sant'Anna and Ecole Doctorale Cerveau-Cognition-Comportement of the University Pierre et Marie Curie, Paris. He was visiting researcher at the at the Laboratoire de Physiologie de la Perception et de l'Action from 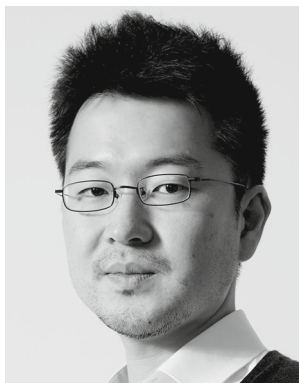February 2010 to June 2010, from April 2011 to July 2011 and from June 2012 to July 2012 under the supervision of Prof. Alain Berthoz. He contributed to the formulation, proposal preparation, and accomplishment of the European project RoboSoM (A Robotic Sense of Movement) from December 2009 to May 2013. He previously contributed in the framework of the RobotCub European project to the implementation of bio-inspired models of eye movements and in the URUS European project to the implementation of a graphic interface for human robot interaction on mobile platforms. His research interests are in the field of humanoid robotics with particular attention to study and implementation of neuroscientific models of sensory-motor coordination.

Nino Cauli is a Postdoctoral Researcher at The BioRobotics Institute, Scuola Superiore Sant'Anna (SSSA) in Pondedera and is a visiting researcher in the VisLab laboratory, part of the Intituto Superior Tecnico in Lisbon. He obtained his Ph.D. student in BioRobotics at the Scuola Superiore Sant'Anna (SSSA) in Pisa in April 2014, under the supervision of Prof. Cecilia Laschi. He graduated in Computer Science at the University of Pisa in 2010. He participated in the RoboSoM European project. He is currently working in the Vinero SP project (sub project of the Human Brain Project). His research interests are in the field of humanoid robotics, machine learning and computer vision with particular attention to the study and implementation of predictive visual sensory-motor systems based on internal models.

Przemyslaw Kryczka is currently a PostDoc researcher at Department of Advanced Robotics at Italian Institute of Technology in Genova, Italy. He received his B.E. degree in 2007 from Warsaw University of Technology in Poland. He received his M.E. in 2011 and Ph.D. degree in 2014 from Waseda University in Japan. His research interests concern all aspects of bipedal robots locomotion, such as dynamic gait planning, stability control, state estimation etc. He is also interested in model based control, distributed control systems and mechatronics in general. He is a member of Robotics Society of Japan and IEEE Robotics and Automation Society.

Kenji Hashimoto is an Assistant Professor of the Research Institute for Science and Engineering, Waseda University, Japan. He received the B.E. and M.E. degrees in Mechanical Engineering from Waseda University, Japan, in 2004 and 2006, respectively. He received the Ph.D. degree in Integrative Bioscience and Biomedical Engineering from Waseda University, Japan, in 2009. While a Ph.D. candidate, he was funded by the Japan Society for the Promotion Science as a Research Fellow. He was a Postdoctoral Researcher at the Laboratoire de Physiologie de la Perception et de l'Action in UMR 7152 Collège de France-CNRS, France from 2012 to 2013. His research interests include walking/running systems, biped robots, and humanoid robots. He is a member of the IEEE, Robotics Society of Japan (RSJ), Japanese Society of Mechanical Engineers (JSME) and Society of Instrument and Control Engineers (SICE). He received the IEEE Robotics and Automation Society Japan Chapter Young Award in 2006, and the JSME Fellow Award for Outstanding Young Engineers in 2008.

Alain Berthoz is Honorary Professor at the College de France, member of the French Academy of sciences and the Academy of Technologies, the Academia Europae, American Academy of Arts and Sciences, and other Academies (Royal Academy of Medicin of Belgium, and Academy of Medicine of Bulgaria). And has received several prizes from severa Academies for his research. He is an Engineer (Ecole des Mines. Nancy), and is an expert in Biomechanics, Psychology and Neurophysiology. He is a world known specialist of the physiology of multisensory integration, spatial orientation, the vestibular system, the oculomotor system, locomotion, and spatial memory. His lab has participated in more than 10 SPACEFLIGHT on the MIR Station, SPACELAB and International Space Station for the study of the influence of gravity on perception, equilibrium and motor control. He cooperates with robotics groups in Japan and Italy for bio-inspired robotics and humanoids and participated in several projects (NEU-ROROBOTICS, ROBOSOM, ROMEO, KOROIBOT etc.). He is the author of more than 300 papers in International journals. Gave plenary lectures at BIOROB, ICRA, IROS. He wrote several books on these subject among which "The Brain's Sense of movement" (Harvard Univ Press), "Emotion and Reason: The cognitive foundations of decision making" (Oxford Univ Press), "Simplexity" (Yale University Press). He has received the honors of Officier de l'Ordre du Mérite, Officier de la Légion d'Honneur, Commandatore of the Order of Merit of the Italian Republic.

Atsuo Takanishi is a Professor of the Department of Modern Mechanical Engineering as well as the director of the Humanoid Robotics Institute, Waseda University. He received the B.S.E. degree in 1980, the M.S.E. degree in 1982 and the Ph.D. degree in 1988, all in Mechanical Engineering from Waseda University. His current researches are related to Humanoid Robotics and its applications in medicine and well-being, such as the biped walking/running humanoids, the emotion expression humanoids, the flute player humanoids, the ultrasound medical inspection robots, the airway management training humanoids, etc. He recently initiated a new mobile robot project for environmental monitoring. He is currently the vice president of the Robotics Society of Japan (RSJ) and of the Japan IFToMM. He is a member of many robotics and medicine related academic societies such as IEEE, RSJ, and the Society of Mastication Systems, etc. He is a fellow of RSJ and the Japanese Society of Mechanical Engineers (JSME). He received the RSJ Best Journal Paper Award (1998), RSJ/JSME ROBOMECH Award (1998), BusinessWeek Best of Asia Award (2001), IROS2003 Best Paper Award—Application (2004), JSME Best Journal Paper Award (2006), ROBIO2007 Best Conference Paper Award (2007) and many more domestic and international awards.

Paolo Dario received his Dr. Eng. Degree in Mechanical Engineering from the University of Pisa, Italy, in 1977. He is currently a Professor of Biomedical Robotics at the Scuola Superiore Sant'Anna (SSSA) in Pisa, where he is the Director of the BioRobotics Institute. He was the founder and Co-ordinator of the ARTS (Advanced Robotics Technology and Systems) Lab and of the CRIM (Center for the Research in Microengineering) Lab of SSSA, now merged into the BioRobotics Institute, where he supervises a team of about 200 researchers and Ph.D. students. He is the Director of Polo Sant'Anna Valdera, the research park of SSSA. From September 2009 to February 2011 he served as the Director of the Center for Micro-BioRobotics IIT@SSSA of the Italian Institute of Technology (IIT). In the years 2002–2003 he served as President of the IEEE Robotics & Automation Society. He is IEEE Fellow and recipient of the Joseph Engelberg Award (1996). He is and has been Visiting Professor at prestigious universities in Italy and abroad, like Brown University, Ecole Polytechnique Federale de Lausanne (EPFL), Waseda University, University of Tokyo, College de France, Zheijang University. His main research interests are in the fields of biorobotics, medical robotics, micro/nanoengineering. He is the coordinator of many national and European projects, the editor of special issues and books on the subject of biorobotics, and the author of more than 450 scientific papers (150 on ISI journals).

Cecilia Laschi is Full Professor of Biorobotics at the BioRobotics Institute of Scuola Superiore Sant' Anna, where she serves as Vice-Director. She received her M.S. in Computer Science from the University of Pisa in 1993 and her Ph.D. in robotics from the University of Genova in 1998. In 2001–2002 she was JSPS visiting researcher at Waseda University in Tokyo. Her research interests are in the field of humanoid and soft biorobotics. She has (co-)authored more than 50 ISI papers (around 200 in total). She is Senior member of the IEEE, of the EMBS, and of the RAS, where she serves as elected AdCom member and Co-Chair of the TC on Soft Robotics.